Biosensors and Bioelectronics 132 (2019) 360–367

Contents lists available at ScienceDirect

Biosensors and Bioelectronics

journal homepage: www.elsevier.com/locate/bios

Label-free strip sensor based on surface positively charged nitrogen-rich carbon nanoparticles for rapid detection of *Salmonella enteritidis*

Zonghan Wang[a], Xiaolin Yao[a], Rong Wang[a], Yanwei Ji[a], Tianli Yue[a], Jing Sun[b], Tao Li[c], Jianlong Wang[a,*], Daohong Zhang[a,*]

[a] College of Food Science and Engineering, Northwest A&F University, 22 Xinong Road, Yangling 712100, Shaanxi, China
[b] Qinghai Key Laboratory of Qinghai-Tibet Plateau Biological Resources, Northwest Institute of Plateau Biology, Chinese Academy of Sciences, Xining 810008, Qinghai, China
[c] Shaanxi institute for Food and Drug Control, Xi'an 710065, Shaanxi, China

ARTICLE INFO

Keywords:
Label free
Lateral flow immunoassay
Surface positively charged nanoparticles
Salmonella enteritidis

ABSTRACT

Lateral flow immunoassay (LFIA) is a class and widespread applied point-of-care biosensor in the rapid monitoring field. To address the matched antibodies and antibody labeling dependence in the conventional LFIAs, in this work, an innovative label-free LFIA was proposed for the sensitive detection of *Salmonella enteritidis* (*S. enteritidis*) by introducing a new nanoparticles-bacteria-antibody sandwich strategy in the sensor. Surface positively charged nitrogen-rich carbon (pNC) nanoparticles, synthesized via calcination and etching reactions, were used as adsorbent to capture bacteria as well as for generating signals. In the presence of target pathogens, bacterial cells could combine with pNC through electrostatic interaction and hydrogen bonding, then the complex would be captured specifically by the anti-bacteria monoclonal antibody (McAb) coated on the test line (T-line). With the accumulation of nanoparticles-bacteria, the color on T-line would be gradually deepened from nearly colorless to deep black. Importantly, the pNC-based immunoassay could exhibit high sensitivity for target pathogens detection with a linear range of 10^2–10^8 cfu mL^{-1} and a low detection limit of 10^2 cfu mL^{-1}. Furthermore, this system was validated preliminarily to screen *S. enteritidis* in different food samples with recoveries ranging from 85% to 110%. Taking advantages of simplicity, label-free, convenience, and sensitivity, the pNC-based LFIA has the application potential for pathogenic microorganisms monitoring in food safety and early clinical diagnosis fields.

1. Introduction

Lateral flow immunoassay is an excellent and classic biosensor broad applied in the rapid pathogens monitoring field, which can achieve favorable sensitivity and selectivity based on antigen-antibody recognition and stable labels. In general, nanoparticles, directly employed as labels for signal readout, can significantly improve the sensitivity and lower the limit of detection (LOD) of biosensors because they can match antibodies (Abs) well and retain the original color properties, such as gold nanoparticles (Bu et al., 2018; Lisa et al., 2009; Liu et al., 2008), carbon nanoparticles (Lee et al., 2012; Yu et al., 2017), quantum dots (Medina-Sanchez et al., 2014; Zou et al., 2010), magnetic nanoparticles (Peterson et al., 2015; Zhang et al., 2013) etc. However, it is generally accepted that the application of these labels is often restricted by either strict synthesis process, chemical instability or complicated cross-linking with Abs of nanomaterials (Zeng et al., 2018). Moreover, the sandwich immunoreaction is frequently employed in bacteria detections, in which two paired Abs are needed to recognize different antigenic determinants and form a sandwich structure (Ngom et al., 2018). In fact, the pairing of Abs is another obstacle because not every Ab can be paired with another through their corresponding antigen (Zeng et al., 2016).

To address these problems, Song and his/her co-workers (Song et al., 2016) presented a label-free direct-type strip sensor, in which by staining target bacteria using fluorescent material, the fluorochrome dye-bacterium complex rather than conventional labeled Ab was applied as a novel signal probe for pathogens detection. Compared with conventional LFIAs, that approach is easy to operate, rapid, portable and exempt from the preparation of traditional labels as well as the time-consuming screening process for paired Abs. Although the current format requires fluorescent staining during the experiment, this LFIA has been further simplified by introducing a new non-matched

* Corresponding authors.
E-mail addresses: wanglong79@nwsuaf.edu.cn (J. Wang), zhangdh@nwsuaf.edu.cn (D. Zhang).

https://doi.org/10.1016/j.bios.2019.02.061
Received 3 December 2018; Received in revised form 18 February 2019; Accepted 20 February 2019
Available online 05 March 2019
0956-5663/

antibody-dependent sandwich strategy. Therefore, exploring a new label-free and non-matched antibody-dependent LFIA is very advantageous for the development of sensitive and convenient technologies in the detection of pathogens. In recent years, advances in nanotechnology have further given new tools for simpler and faster pathogens detection, e.g., some studies have demonstrated that the functionalized nanoparticles can aggregate on bacterial surface. Li et al. (2013) developed an attractive system based on a positively charged graphene oxide-enzyme complex for bacteria detection. Furthermore, the antimicrobial activity of the iron oxide nanoparticles coated with chitosan was investigated by Arakha et al. (2015). Such superior property of nanoparticles is highly desired to researchers for pathogen detections.

Herein, we firstly proposed and introduced a nanoparticles-bacteria-antibody sandwich strategy to replace the conventional Ab_1-bacteria-Ab_2 sandwich pattern and designed a new label-free LFIA method for the ultra-sensitive, specific, rapid and cost-effective detection of pathogens. Currently, the foodborne pathogenic bacterium is still a major public health threat to countries all around the world. Among these pathogens, *Salmonella enteritidis* (*S. enteritidis*) is one of the most widely found pathogens causing food borne disease (Lipkin, 2013; Singh et al., 2015). It is reported that about 86% (80.3 million/93.8 million) of foodborne diseases are caused by *Salmonella* leading to 155,000 deaths annually (Havelaar et al., 2015). Here, *S. enteritidis* was selected as the target bacteria to demonstrate the new strategy, where *S. enteritidis* could combine with surface positively charged nitrogen-rich carbon nanoparticles, and then captured specifically by the anti-bacteria McAb coated on T-line beforehand. In the pNC-based strip sensor, only one unlabeled Ab was used to detect *S. enteritidis* successfully with excellent sensitivity and selectivity, which not only got rid of a series of troublesome marking steps providing an unexpected alternative to traditional probes, but also avoided the use of paired McAbs obtained by a time-consuming screening process. Also, to demonstrate the feasibility of the biosensor, a proof-of-concept assay for *S. enteritidis* detection in potable water, cole slaw cabbage salad, watermelon juice and purple cabbage salad samples were performed with a low LOD. Results indicated that the pNC-based label-free LFIA method held considerable promise as a simple, rapid, and cost-effective biosensor for food pathogens detection.

2. Materials and methods

2.1. Reagents and chemicals

A McAb to target *S. enteritidis* flagellin was prepared in our laboratory as previously reported (Zhang et al., 2011), and the assay performances of the McAb had been characterized by enzyme-linked immunosorbent assay (ELISA). The preparation process and characterization results of the McAb were listed in Supporting information. Nitrocellulose (NC) membranes were purchased from Millipore Corp. Glass fibers, sample pads, and absorbent pads were purchased from Shanghai Kingdiag-biotech CO., Ltd. Bovine serum albumin (BSA) was obtained from MP Biochina. Luria-Bertani (LB) medium was purchased from Beijing Land Bridge Technology Co., China. Urea was purchased from Beijing Solarbio Science & Technology Co., Ltd (Beijing, China). Nitric acid (HNO_3) was purchased from Kelong Chemical Reagent Co., Ltd. (Chengdu, China). 1,4-benzenedicarboxylic acid and triethylenediamine were purchased from Aladdin chemistry Co. Ltd. (Shanghai, China). All solvents and other chemicals used in this work were of analytical-reagent grade or better.

2.2. Equipment

Guillotine cutter (HGS-201) was purchased from Hangzhou Autokun Technology Co., Ltd. The high speed refrigerated centrifuge (HC-3018R) was obtained from Anhui USTC Zonkia Scientific Instruments Co., Ltd. Freeze dryer (FDS-2.5E) was purchased from SIM International Group Co., Ltd. The shaker and heating oven were purchased from Shanghai Jinghong Laboratory Equipment Co., Ltd. The morphology of the nanoparticles was characterized with scanning electron microscopes (SEM) named Hitachi S-4800. The Fourier-transform infrared (FTIR) spectrum was recorded with a Vetex 70 (Bruker Corp, Germany). The zeta potentials of nanoparticles and bacterial suspension were evaluated using Zetasizer Nano-ZS instrument (Malvern, UK). Transmission electron microscopy (TEM) measurements were performed on a HT7700 (Hitachi, Japan) at 80 kV.

2.3. Bacterial strains

The following microorganisms as food-borne pathogenic bacteria were used in this study including *Salmonella enteritidis* ATCC13076, *Salmonella typhimurium* ATCC 43174, *Salmonella paratyphi B* ATCC10719, *Salmonella london* ATCC 8389, *Salmonella hadar* ATCC51956, *Escherichia coli* O157:H7 ATCC 43889, *Staphylococcus aureus* ATCC 12600, *Enterobacter sakazakii* ATCC29004, *Listeria monocytogenes* ATCC19114, *Campylobacter jejuni* ATCC43461 and *Candida albicans* ATCC96268. All these microorganisms were purchased from Shanghai Prajna biology technique Co. Ltd (Shanghai, China). The strains were transferred into LB liquid medium and cultured at 37 °C for 18–24 h before further use (Ben Aissa et al., 2017). Then, the bacteria stock solutions were diluted to the testing concentration.

2.4. Synthesis of the pNC

The pNC nanoparticles were prepared via direct calcination and etching (Scheme 1a). Specifically, urea was put into a covered crucible, heated over 4 h to 550 °C in air and kept at this temperature for another 4 h. The as-formed yellow solid was the g-C_3N_4 which was then ground into powder for further use. The homogeneous precursor solution was prepared by dissolving 1,4-benzenedicarboxylic acid (302 mg) and triethylenediamine (216 mg) in 30 mL of dimethylformamide (DMF). Then the g-C_3N_4 powder (2.06 g) was added to the mixed DMF solution under magnetic stirring. After removing the solvent, the solid powder was transferred to a tube furnace, heated to 800 °C at a rate of 1.5 °C min^{-1} under an Ar atmosphere and maintained at this temperature for 1 h. The as-obtained black solid powder was nitrogen-rich carbon nanoparticles (NC). Then, 1 g of NC powder was put into 100 mL 5 M HNO_3 and refluxed for 24 h at 125 °C. After naturally cooling to room temperature, the refluxed product was centrifuged and washed with ultrapure water until its pH reached 7.0. The final product was vacuum dried at 35 °C for 12 h to obtain surface positively charged nitrogen-rich carbon nanoparticles (pNC). The final product was used for further characterizations and experiments.

2.5. Fabrication of the LFIA strip

The LFIA biosensor was made of sample pad, conjugate release pad, nitrocellulose filter membrane and absorbent pad. The absorbent pad was used as received without further modification. The sample and conjugate pads were treated with blocking buffer of 2% BSA in 10 mM PBS (pH 7.4) and dried at 37 °C overnight. Detection McAb (1 mg mL^{-1}), at a rate of 1 μL cm^{-1}, was dispensed on the nitrocellulose filter membrane to form the T line. The nitrocellulose filter membrane was then dried for 30 min at room temperature. After that, the test strip was assembled by sequentially adhering the absorbent pad, nitrocellulose filter membrane, conjugate pad, and sample pad onto a PVC sheet with about 2 mm overlapping. Finally, the strip was cut into 3 mm width and stored in a desiccator.

2.6. Procedure of the LFIA strip sensor

To investigate the practicality of this new sandwich strategy, 100 μL standard *S. enteritidis* solution of varying concentrations between 0 and

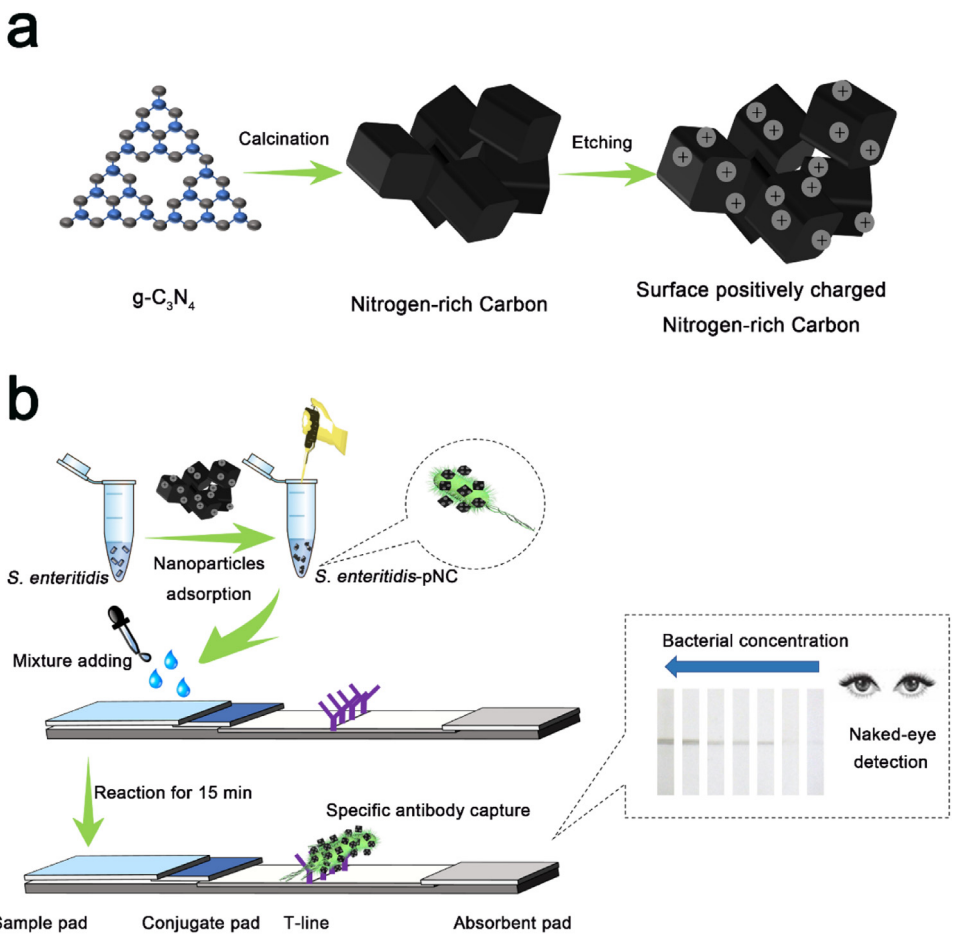

Scheme 1. Schematic illustrations of (a) preparation of pNC, (b) S. enteritidis detection by the pNC-LFIA sensor.

10^8 cfu mL^{-1} was separately incubated with pNC for a period of time at 37 °C. Then the mixture was dipped onto the sample pad of test strip to start the chromatography assay. After 15 min, the images of test strips were photographed by a Cannon digital camera and then processed using Image J to analyze the signal intensity of T-line. To elaborate the changes of signal, the mean gray value of optical density was calculated in the area corresponding to T line of the test strip with the Image J software. Each test was repeated for at least 3 times (n ≥ 3) under the same condition.

2.7. S. enteritidis detection in food samples by the pNC based LFIA strip

Potable water, cole slaw cabbage salad, watermelon juice and purple cabbage salad were obtained from a local supermarket and confirmed to be free of *Salmonella* spp. by the culture-based method. Watermelon juice and potable water were stored at 4 °C. Ten grams of crushed cole slaw cabbage salad and purple cabbage salad samples were aseptically added to a flask, mixed with 90 mL of PBS, respectively. The flasks were sonicated for 5 min and vortexed vigorously. The mixtures were then incubated overnight at 4 °C for further use. Finally, all food samples were centrifuged to remove food debris (Shukla et al., 2014). The supernatants were sterilized by high-temperature sterilization, filtrated through a 0.22 μm-membrane filter and artificially contaminated with *Salmonella* to obtain different final bacterial concentrations of 0–10^8 cfu mL^{-1} (Bayrac et al., 2017). The experiments were conducted in triplicate.

3. Results and discussion

3.1. Principles of the pNC synthesis and the pNC-based LFIA strip sensor

The synthesis principle of the pNC and the operating principle of the pNC-based LFIA strip for *S. enteritidis* detection are schematically depicted in Scheme 1. For efficiently and rapidly capturing bacteria, we prepared the pNC by two main steps: calcination and etching, as illustrated in Scheme 1a. In this process, some low-cost organic molecules (terephthalic acid and triethylenediamine) were used as the precursors and graphitic carbon nitride powder (bulk phase) was used as the main nitrogen source.

Scheme 1b schematically illustrates the detection process of *S. enteritidis* by this novel label-free LFIA strip sensor. During the assay, pNC nanoparticles were first added into bacterial suspension of *S. enteritidis*. Immediately, pNC would be adsorbed onto the surface of *S. enteritidis*. Then the pNC-*S. enteritidis* complex was added to sample pad and migrated along the sample pad toward conjugate pad driven by the capillary action. When the complex solution reached nitrocellulose filter membrane, the complex would be retained by the pre-coated detection McAb because of the specific antibody-antigen interaction between McAb and *S. enteritidis*. With the accumulation of *S. enteritidis*-nanoparticles, the color on T-line would be gradually deepened. If there were target bacteria in the sample, a characteristic brown band could be observed. Correspondingly, no band would appear on the T-line if no *S. enteritidis* was present in the sample. By this strategy, *S. enteritidis* would be successively captured and effectively detected by nanoparticles and McAb. The nanoparticles-bacteria-antibody sandwich pattern skillfully replaced the conventional sandwich immunoassay format that was obliged to adopt detection and capture Abs

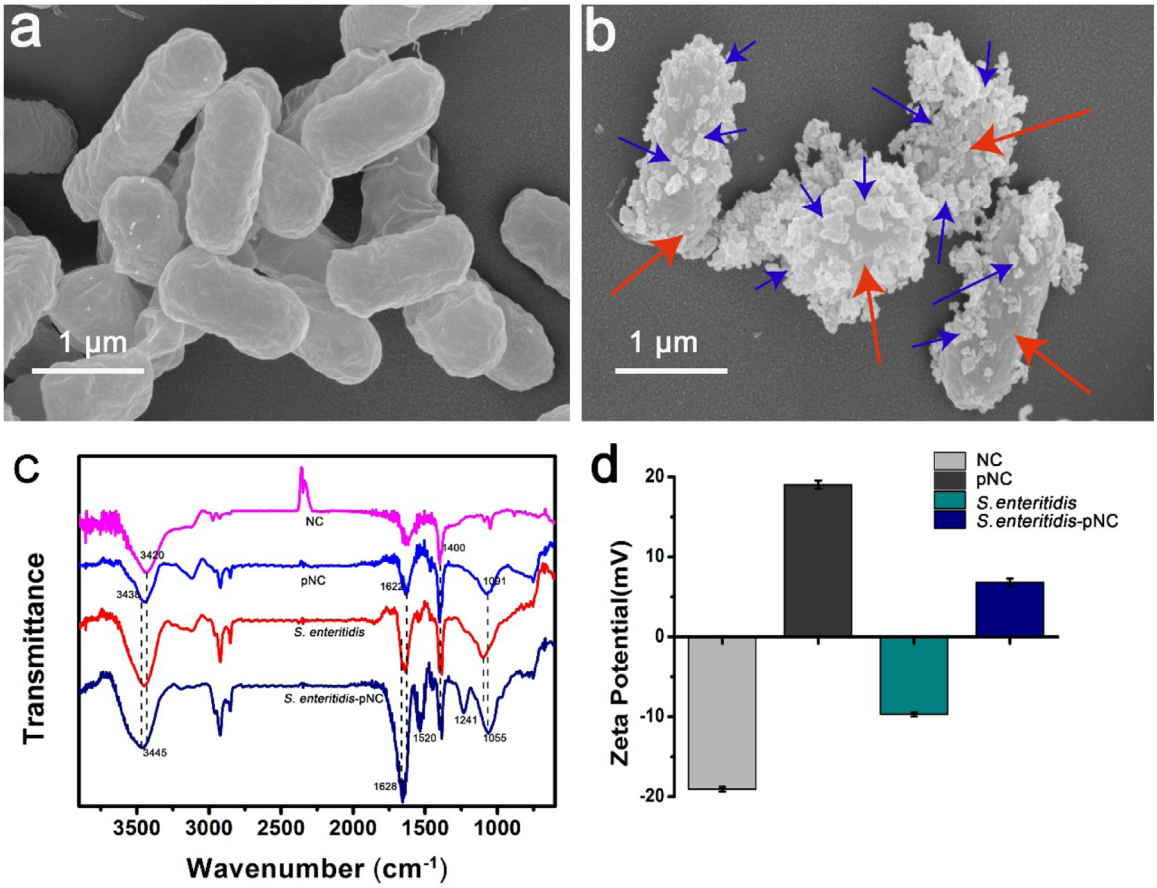

Fig. 1. Investigation results of conjugating capacity of pNC toward bacteria. (a) SEM image of bacterial suspension (b) SEM image of pNC (red arrows) conjugated *S. enteritidis* (blue arrows) (c) FT-IR spectroscopy of NC, pNC, pNC-*S. enteritidis* complex and *S. enteritidis* (d) Zeta potential of the dispersions of NC, pNC, *S. enteritidis* and pNC-*S. enteritidis* complex. (For interpretation of the references to color in this figure legend, the reader is referred to the web version of this article).

simultaneously.

3.2. Capability to capture bacteria of the pNC

As shown in Fig. 1b, after the addition of pNC into bacterial suspension, *S. enteritidis* featured a large number of small aggregates resulting from the evenly dispersion of pNC over the whole surface of bacterium. Control micrograph of *S. enteritidis* is presented in Fig. 1a. Such results indicate that pNC has the interaction capability with *S. enteritidis*. Fig. 1c displays the fourier transform infrared (FT-IR) spectra of the NC, pure pNC, pNC-*S. enteritidis* complex and *S. enteritidis*. For pure NC, the broad band around 3420 cm^{-1} is assigned to stretching of -OH and -NH_2 groups (Aziz and Salama, 2018), while the band at 1400 cm^{-1} is due to C-N stretching (Ding et al., 2018). Remarkably, a new peak emerges at 1055 cm^{-1}, which is attributed to the carboxyl function group of pNC, indicating the presence of new functional groups after modification (Bao and Li, 2012). In the case of the pNC-*S. enteritidis* complex, the characteristic bands for pNC still remain, but slight changes can be observed as compared with those of the pure pNC and bacteria: the peaks at 1055 and 3445 cm^{-1} shift to 1091 and 3438 cm^{-1}, respectively. Moreover, the band at 1622 cm^{-1} shift to 1628 cm^{-1} owing to C=O stretching (Demiral and Gungor, 2016). Significantly, two new bands appear at 1520 cm^{-1} and 1241 cm^{-1} due to the NH_2 scissoring and stretching modes of CN heterocycles, respectively (Singh et al., 2011; Xiang et al., 2011). It is presumably ascribed to the formation of hydrogen bond between NH_2 and COOH, confirming the strong interaction between bacteria and nanoparticles.

To further verify the adsorption mechanism, zeta potential measurements were carried out. Evidently, the zeta potential value of pNC was measured to be + 19.1 mV when dispersed in water as compared to that of −19.0 mV for pristine NC as a result of protonation. Moreover, the surface of bacteria is always negatively charged (Fig. 1d). Thus, after the addition of nanoparticles to the bacteria, the surface positively charged nitrogen-rich carbon nanoparticles clustered onto the bacterial surface through complementary electrostatic interactions (Zhao et al., 2018).

3.3. Optimization of experimental conditions

In this study, the effects of detection conditions (incubation time, pNC concentration and pH of bacterial suspension) on the experimental results were explored. All these parameters were optimized using a *S. enteritidis* standard solution of 10^7 cfu mL^{-1}. As a key factor for most LFIAs, the influence of incubation time on the color development of strip's T-line was examined. The mixture of pNC and bacteria was allowed to incubate for 0, 5, 10, 15, 20 and 25 min, respectively. As shown in Fig. 2a, with the increase of incubation time, the color intensity on T-line deepened gradually until the time reached 5 min, and thereafter kept at an almost constant level. Considering the fact that the nanoparticles can combine with bacteria by hydrogen bonding and electrostatic interaction quickly, 5 min was considered to be the optimal incubation time in subsequent experiments. Furthermore, the color development on T-line of the strip was examined under different concentrations (0.05–0.55 mg mL^{-1}) of pNC separately dispersed into 100 μL bacterial suspension. As shown in Fig. 2b, with the increase of adsorbent amount, the color intensity on T-line deepened gradually and reached a maximum at 0.35 mg mL^{-1}. Thus, 0.35 mg mL^{-1} of pNC was screened out for the further experiment. Besides, pH of bacterial

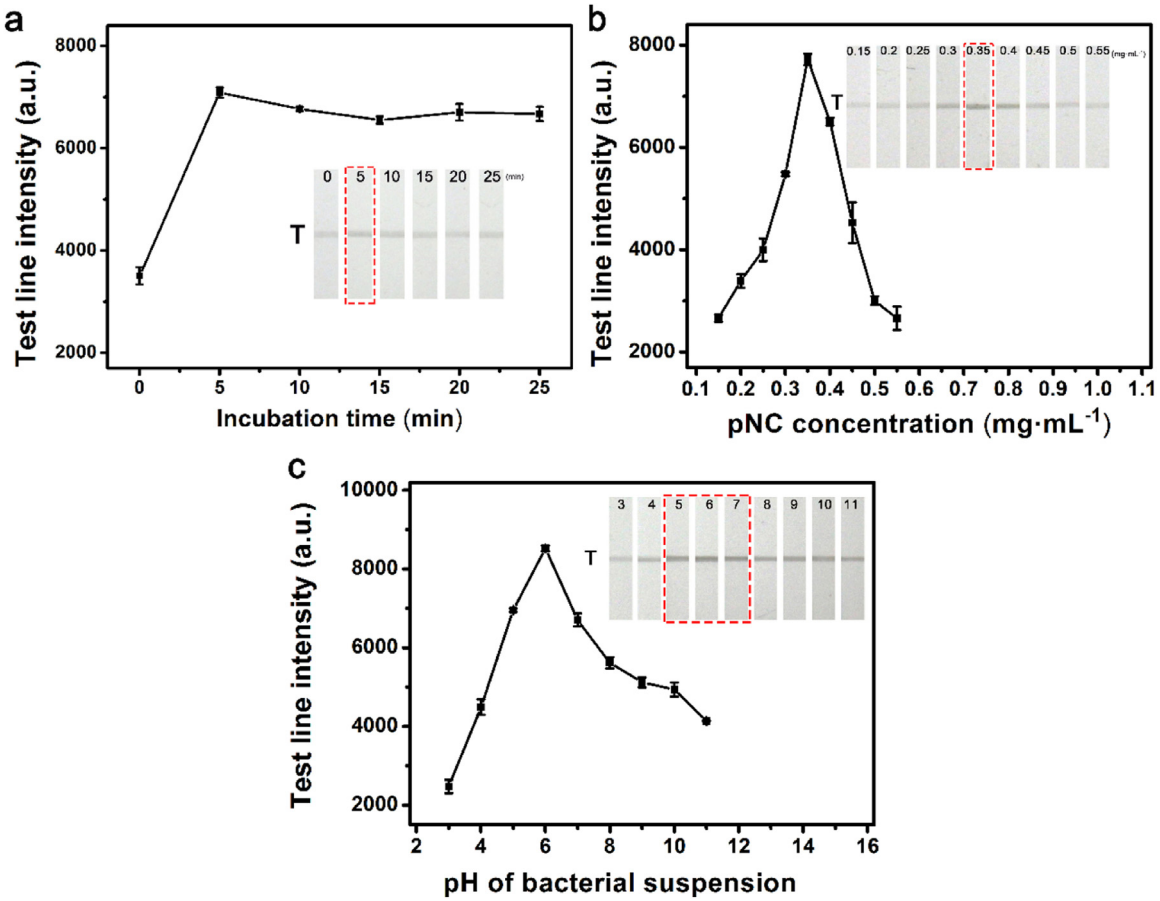

Fig. 2. Effects of (a) incubation time, (b) concentration of pNC and (c) pH of bacterial suspension on LFIA responses to *S. enteritidis* of 10^7 cfu mL^{-1} (inset images: results for optimization tests; red rectangular boxes: the optimal conditions chosen for further experiments). (For interpretation of the references to color in this figure legend, the reader is referred to the web version of this article).

suspension is of vital importance to this process, which is benefit to guarantee reliability of results and improve detection sensitivity. To achieve an optimal signal, pH value of bacterial suspension was investigated. As shown in Fig. 2c, when the pH value of bacterial suspension is around 5.0–7.0, the color of T-line doesn't make much difference and can reach higher intensity than those of other pH values. So, a weak acidic to neutral surrounding around pH 5.0–7.0 was beneficial to the analysis and could be used as appropriate conditions for test throughout this study.

3.4. Analytical performance

Sensitivity and specificity are important parameters to evaluate the performance of a new proposed LFIA. Briefly, based on the above optimized detection conditions, the sensitivity of the proposed platform was determined with standard *S. enteritidis* at concentrations of 10^1–10^8 cfu mL^{-1} in 10 mM PBS (pH 7.4), with PBS as the negative control. From the results of Fig. 3a, we found that with an increase of target *S. enteritidis* in the detection solution, the intensity on the T-line increased. Furthermore, when the *S. enteritidis* was 10^1 cfu mL^{-1}, the intensity of the brown band on T-line was basically no difference with that of the negative control strip, and 10^2 cfu mL^{-1} was the minimum bacterial concentration that could make a difference in color intensity with that of the negative control strip. Herein, 10^2 cfu mL^{-1} could be treated as the visual LOD of this LFIA. The corresponding optical densities were further confirmed by recording their values of color bands on the test zone with Image J software. Moreover, the peak area on T-line was found to be directly proportional to the logarithm of S. enteritidis concentrations. In concentrations ranging from 10^2 to 10^8 cfu mL^{-1}, the calibration curve was y = 1434x–2340. (Fig. 3b).

To further confirm the improvement of the pNC based LFIA in the assay performance, serial concentrations of *S. enteritidis* were also analyzed by the pure NC based LFIA. As shown in Fig. 3c, LOD of the NC-based LFIA was 10^5 cfu mL^{-1}. To our delight, the pNC based LFIA showed an improvement of at least 1000-fold in sensitivity than that of the NC-based LFIA. There was a strong possibility that the efficient performance of pNC was attributed to the hydrogen bonding and electrostatic interaction compared with that of pure NC. Besides, the comparison results showed that the assay performance of the pNC based LFIA here could rival or surpass those of the previously reported LFIAs for bacteria detection (Table 1).

The nanoparticles-bacteria-antibody sandwich strategy was introduced with pNC as the bacteria recognition agent to capture the whole cell of *S. enteritidis*. As a surface positively charged nanoparticle, pNC shows noticeable affinity to many types of bacteria. In this light, it possessed universality but lacked of specificity with this kind of nanoparticles as recognition agents in bacteria detection. To offer selectivity and ensure application reliability, anti-*S. enteritidis* IgG which could specific interact with flagellin of *S. enteritidis* was selected as the second recognizing factor. The two recognition agents bound with *S. enteritidis* at two distinct sites, thus, a complementary effect between the screening difficulty of paired McAbs and specificity deficiency of nanoparticles could be easily achieved. To validate the specificity of the biosensor, cross reaction experiments were carried out with four *Salmonella* strains including *Salmonella london* (*S. london*), *Salmonella typhimurium* (*S. typhimurium*), *Salmonella paratyphi B* (*S. paratyphi B*) and *Salmonella hadar* (*S. hadar*), and five non-*Salmonella* strains of *Staphylococcus aureus* (*S. aureus*), *Escherichia coli* (*E. coli*), *Candida*

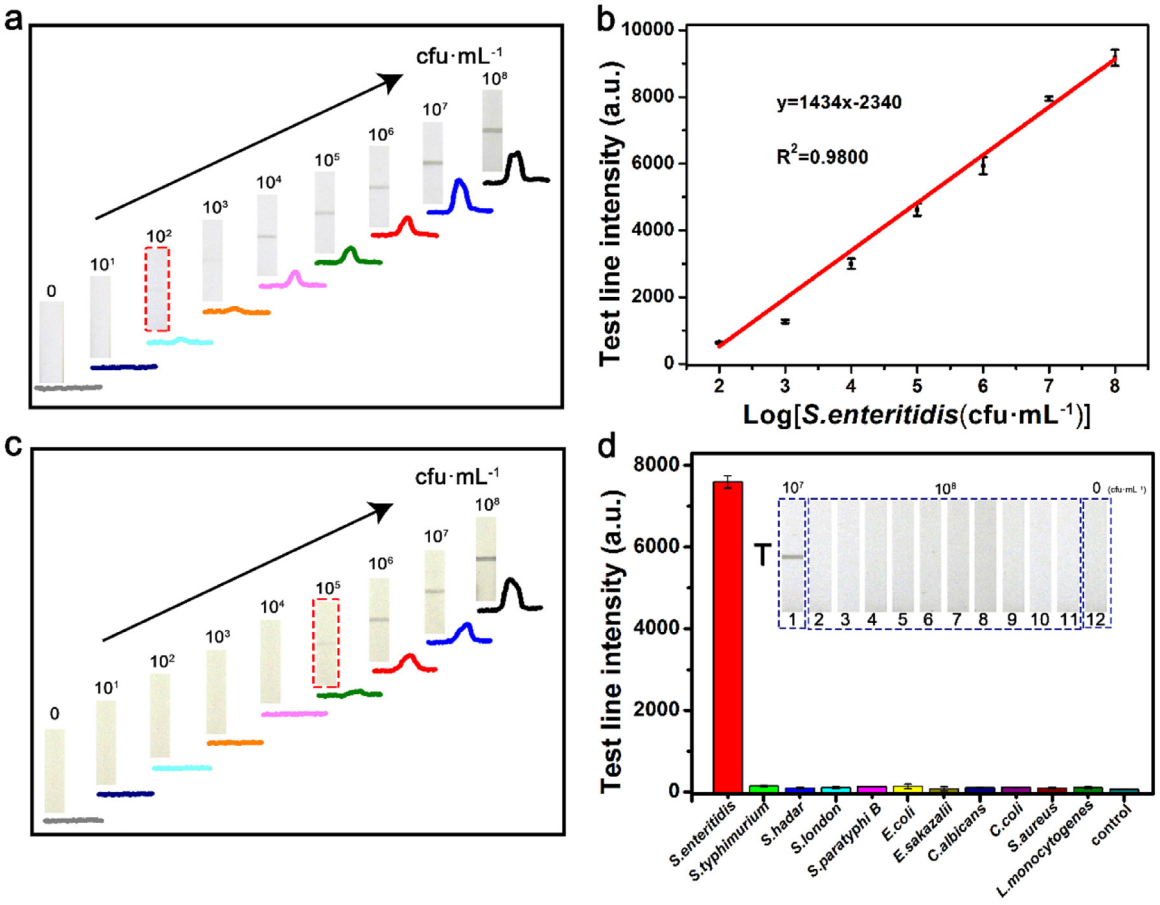

Fig. 3. Assay performances for *S. enteritidis* detection. (a) Results for sensitivity test by the pNC-based LFIA. (b) Calibration curve of *S. enteritidis* detection using the pNC-based LFIA. (c) Results for sensitivity test by the NC-based LFIA. (d) Specificity research results to different interfering bacterial strains (No. 1 corresponds to 10^7 cfu mL^{-1} of S. enteritidis, 2–11 correspond to 10^8 cfu mL^{-1} of *S. london*, *S. typhimurium*, *S. paratyphi B*, *S. hadar*, *S. aureus*, *E. coli*, *C. albicans*, *L. monocytogenes* and *C. coli*, respectively, 12 corresponds to the control strip).

albicans (*C. albicans*), *Listeria monocytogenes* (*L. monocytogenes*) and *Campylobacter coli* (*C. coli*) as the interference pathogens, respectively, with PBS as the negative control. As seen in Fig. 3d, although with a 10 times higher concentration (10^8 cfu mL^{-1}), no obvious signals can be observed on T-line of strips for these interfering pathogens compared to that of the strip for *S. enteritidis* (10^7 cfu mL^{-1}), displaying an acceptable selectivity of the proposed sensor.

Furthermore, since *Salmonella* is a kind of gram-negative bacteria. To investigate the universal applicability of the strategy to other bacteria, *L. monocytogenes,* a kind of gram-positive bacteria, was selected as another model target and detected using the proposed pNC based strip sensor. The related results (Fig. S4) demonstrated that the developed strip sensor could also be used for *L. monocytogenes* detection with a high sensitivity (10^3 CFU mL^{-1}) and selectivity. So, it can be declared that by coating corresponding detection Abs, the pNC based strip sensor has a universal applicability in the detection of pathogen bacteria.

3.5. Application in food samples

To demonstrate the applicability of this introduced biosensor in

Table 1
Comparison of sensitivity for pathogen detections by different LFIA devices.

Bacteria analyte	Type of label	LOD[a] (cfu mL^{-1})	Reference
Y. pestis and *B. pseudomallei*	Up-converting phosphor (UCP)	10^3	(Liang et al., 2017)
Salmonella choleraesuis	Gold magnetic bifunctional nanobeads	5×10^5	(Xia et al., 2016)
Escherichia coli O157	gold nanoparticles	10^5	(Park et al., 2016)
S. typhimurium		10^6	
Enterobacter cloacae	gold nanoparticles	10^2	(Zhang et al., 2016)
Listeria monocytogenes	Surface-enhanced Raman scattering (SERS)	1.9×10^2	(Liu et al., 2017)
S. enteritidis	Horseradish peroxidase (HRP)	2.7×10^2	(Eltzov and Marks, 2017)
Escherichia coli	Cell wall binding domains (CBDs)	10^2	(Kong et al., 2017)
Bacillus cereus	Eu(III)-doped polystyrene nanoparticle (EuNP)	10^4	(Xing et al., 2018)
E.coli O157:H7	Streptavidin-QD 655	10^6	(Morales-Narvaez et al., 2015)
Escherichia coli	Bacteriophage amplification	10^1 (standard buffer)	
Escherichia coli	**Label-free**	10^2 (bottled water and milk)	(Alcaine et al., 2016)
S. enteritidis		10^3	**This work**
		10^2	

[a] LOD, limit of detection.

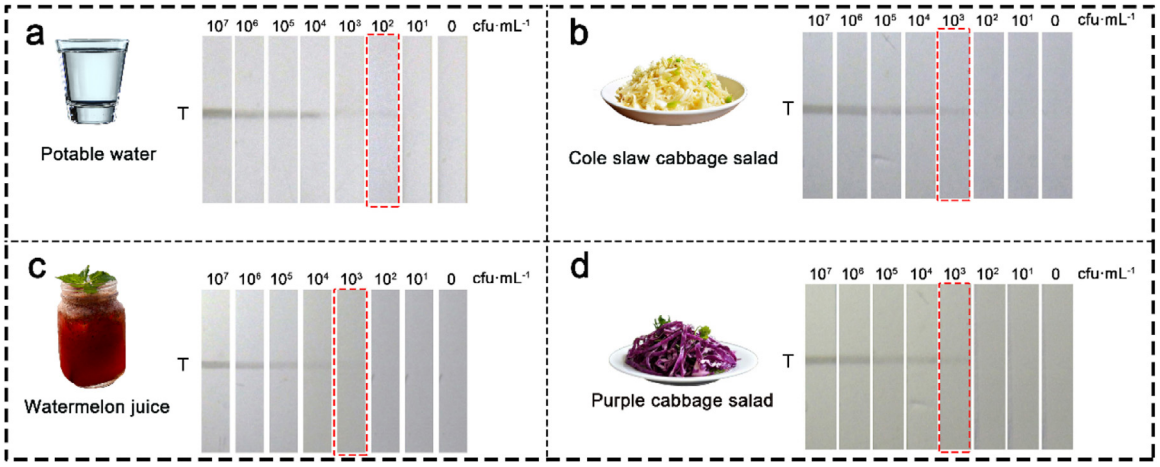

Fig. 4. Detection results of *S. enteritidis* in food samples by the pNC-based LFIA biosensor.

Table 2
Recovery efficiency of *S. enteritidis* spiked in food samples based on the proposed strategy.

Sample	Spiked (cfu mL^{-1})	Found (cfu mL^{-1})	Recovery (%)	RSD[a] (%, n = 3)
potable water	1.0×10^3	9.3×10^2	93	2.9
cole slaw cabbage salad	1.0×10^4	9.5×10^3	95	4.3
watermelon juice	1.0×10^6	9.6×10^5	96	3.1
purple cabbage salad	1.0×10^7	1.1×10^7	110	2.3
	1.0×10^3	1.1×10^3	110	5.3
	1.0×10^4	9.8×10^3	98	4.7
	1.0×10^6	8.5×10^5	85	6.2
	1.0×10^7	9.0×10^6	90	6.6
	1.0×10^3	8.7×10^2	87	4.2
	1.0×10^4	8.9×10^3	89	3.8
	1.0×10^6	9.2×10^5	92	3.1
	1.0×10^7	8.5×10^6	85	2.6
	1.0×10^3	9.3×10^2	93	7.2
	1.0×10^4	9.5×10^3	95	4.8
	1.0×10^6	9.8×10^5	98	7.3
	1.0×10^7	9.0×10^6	90	6.4

[a] RSD, relative standard deviation.

food samples, potable water, cole slaw cabbage salad, watermelon juice and purple cabbage salad were used as complex food samples (Nahim-Granados et al., 2018). Generally, the samples were spiked with *S. enteritidis* and treated according to the procedure described in Section 2.7. As illustrated in Fig. 4, when the spiked concentration decreased, the color intensities on T-line faded gradually. This phenomenon was well agreed with that of the standard bacterial suspension described above. The minimum addition concentrations of bacterial suspension that made the T-line significantly darker than those of the negative control strips were 10^2 cfu mL^{-1}, 10^3 cfu mL^{-1}, 10^3 cfu mL^{-1} and 10^3 cfu mL^{-1} respectively for four kinds of food matrices (Fig. 4a to d), indicating that the method was valid for *S. enteritidis* detection in food samples with no or little matrix effect on the results. Furthermore, the measurement accuracy of *S. enteritidis* in food samples was also evaluated by determining the recovery of spiked bacteria via a standard addition method (where low, medium, and high levels of standard analyte solutions were added to the tested samples). As shown in Table 2, the average recoveries of spiked *S. enteritidis* were between 85% and 110% with RSD values all below 7.3%, demonstrating satisfying application potential and favorable reproducibility of the biosensor for *S. enteritidis* detection in food samples.

4. Conclusion

Here, a pNC based strip biosensor has been developed for the detection of *S. enteritidis*. This biosensor has a LOD of 10^2 cfu·mL^{-1} with a linear range from 10^2 to 10^8 cfu mL^{-1}. Compared with existing methods, the merits of the assay are that: (1) differing from the traditional marking materials, the pNC here is not only used to generate signal but also used to capture bacteria by forming a new sandwich format; (2) only single Ab is needed to obtain comparable or better results than traditional sandwich format; (3) the new LFIA has an universal applicability in the detection of pathogen bacteria; (4) the fabrication process of the pNC-based LFIA is cost-effective, rapid, simple and labor-saving. The pity is that no enough corresponding specific Abs can be supplied currently in our group, which limited the popularization of this method. So, more specific anti-bacteria Abs will be developed in the future to extend this method.

CRediT authorship contribution statement

Zonghan Wang: Conceptualization, Methodology, Formal analysis, Writing - original draft. **Xiaolin Yao:** Validation. **Rong Wang:** Investigation. **Yanwei Ji:** Resources. **Tianli Yue:** Resources. **Jing Sun:** Funding acquisition. **Tao Li:** Funding acquisition. **Jianlong Wang:** Conceptualization, Writing - review & editing, Supervision, Project administration. **Daohong Zhang:** Conceptualization, Writing - review & editing, Supervision, Project administration.

Acknowledgments

The authors thank the National Natural Science Foundation of China (21675127), the Natural Science Foundation of Qinghai Province (No.2019-ZJ-904), Development Project of Qinghai Key Laboratory (No. 2017-ZJ-Y10), Capacity Building Project of Engineering Research Center of Qinghai Province (2017-GX-G03) and the Shaanxi Provincial Science Fund for Distinguished Young Scholars (2018JC-011).

Declaration of interests

None.

Appendix A. Supplementary material

Supplementary data associated with this article can be found in the online version at doi:10.1016/j.bios.2019.02.061.

References

Alcaine, S.D., Law, K., Ho, S., Kinchla, A.J., Sela, D.A., Nugen, S.R., 2016. Biosens. Bioelectron. 82, 14–19.

Arakha, M., Pal, S., Samantarrai, D., Panigrahi, T.K., Mallick, B.C., Pramanik, K., Mallick, B., Jha, S., 2015. Sci. Rep. 5, 12.

Aziz, M.S.A., Salama, H.E., 2018. Int. J. Biol. Macromol. 116, 840–848.

Bao, L.H., Li, X.D., 2012. Adv. Mater. 24 (24), 3246–3252.

Bayrac, C., Eyidogan, F., Oktem, H.A., 2017. Biosens. Bioelectron. 98, 22–28.

Ben Aissa, A., Jara, J.J., Sebastian, R.M., Vallribera, A., Campoy, S., Pividori, M.I., 2017. Biosens. Bioelectron. 88, 265–272.

Bu, T., Huang, Q., Yan, L.Z., Huang, L.J., Zhang, M.Y., Yang, Q.F., Yang, B.W., Wang, J.L., Zhang, D.H., 2018. Food Control 84, 536–543.

Demiral, H., Gungor, C., 2016. J. Clean. Prod. 124, 103–113.

Ding, X.H., Pan, S.M., Lu, C., Guan, H.M., Yu, X.W., Tong, Y.J., 2018. Mater. Lett. 228, 5–8.

Eltzov, E., Marks, R.S., 2017. Biosens. Bioelectron. 87, 572–578.

Havelaar, A.H., Kirk, M.D., Torgerson, P.R., Gibb, H.J., Hald, T., Lake, R.J., Praet, N., Bellinger, D.C., De Silva, N.R., Gargouri, N., Speybroeck, N., Cawthorne, A., Mathers, C., Stein, C., Angulo, F.J., Devleesschauwer, B., World Hlth Org Foodborne Dis, 2015. PLos Med. 12 (12), 23.

Kong, M., Shin, J.H., Heu, S., Park, J.K., Ryu, S., 2017. Biosens. Bioelectron. 96, 173–177.

Lee, J.S., Joung, H.A., Kim, M.G., Park, C.B., 2012. ACS Nano 6 (4), 2978–2983.

Li, J., Wu, L.J., Guo, S.S., Fu, H.E., Chen, G.N., Yang, H.H., 2013. Nanoscale 5 (2), 619–623.

Liang, Z.Q., Wang, X.C., Zhu, W., Zhang, P.P., Yang, Y.X., Sun, C.Y., Zhang, J.J., Wang, X.R., Xu, Z., Zhao, Y., Yang, R.F., Zhao, S.L., Zhou, L., 2017. ACS Appl. Mater. Interfaces 9 (4), 3497–3504.

Lipkin, W.I., 2013. Nat. Rev. Microbiol. 11 (2), 133–141.

Lisa, M., Chouhan, R.S., Vinayaka, A.C., Manonmani, H.K., Thakur, M.S., 2009. Biosens. Bioelectron. 25 (1), 224–227.

Liu, B.H., Tsao, Z.J., Wang, J.J., Yu, F.Y., 2008. Anal. Chem. 80 (18), 7029–7035.

Liu, H.B., Du, X.J., Zang, Y.X., Li, P., Wang, S., 2017. J. Agric. Food Chem. 65 (47), 10290–10299.

Medina-Sanchez, M., Miserere, S., Morales-Narvaez, E., Merkoci, A., 2014. Biosens. Bioelectron. 54, 279–284.

Morales-Narvaez, E., Naghdi, T., Zor, E., Merkoci, A., 2015. Anal. Chem. 87 (16), 8573–8577.

Nahim-Granados, S., Perez, J.A.S., Polo-Lopez, M.I., 2018. Catal. Today 313, 79–85.

Ngom, B., Guo, Y.C., Wang, X.L., Bi, D.R., 2018. Anal. Bioanal. Chem. 410 (11) (2859-2859).

Park, J., Shin, J.H., Park, J.K., 2016. Anal. Chem. 88 (7), 3781–3788.

Peterson, R.D., Chen, W.L., Cunningham, B.T., Andrade, J.E., 2015. Biosens. Bioelectron. 74, 815–822.

Shukla, S., Leem, H., Lee, J.S., Kim, M., 2014. Can. J. Microbiol. 60 (6), 399–406.

Singh, J., Sharma, S., Nara, S., 2015. Food Chem. 170, 470–483.

Singh, S., Barick, K.C., Bahadur, D., 2011. J. Hazard. Mater. 192 (3), 1539–1547.

Song, C.M., Li, J.W., Liu, J.X., Liu, Q., 2016. Talanta 156, 42–47.

Xia, S.Q., Yu, Z.B., Liu, D.F., Xu, C.L., Lai, W.H., 2016. Food Control 59, 507–512.

Xiang, Q., Yu, J., Jaroniec, M., 2011. J. Phys. Chem. C 115 (15), 7355–7363.

Xing, K.Y., Peng, J., Liu, D.F., Hu, L.M., Wang, C., Li, G.Q., Zhang, G.G., Huang, Z., Cheng, S., Zhu, F.F., Liu, N.M., Lai, W.H., 2018. Anal. Chim. Acta 998, 52–59.

Yu, L., Li, P.W., Ding, X.X., Zhang, Q., 2017. Talanta 165, 167–175.

Zeng, H.J., Guo, W.B., Liang, B.B., Li, J.W., Zhai, X.Z., Song, C.M., Zhao, W.J., Fan, E.G., Liu, Q., 2016. Anal. Bioanal. Chem. 408 (22), 6071–6078.

Zeng, H.J., Zhai, X.Z., Xie, M.M., Liu, Q., 2018. Plant Dis. 102 (3), 527–532.

Zhang, D.H., Li, P.W., Yang, Y., Zhang, Q., Zhang, W., Xiao, Z., Ding, X.X., 2011. Talanta 85 (1), 736–742.

Zhang, X., Wang, H.B., Yang, C.M., Du, D., Lin, Y.H., 2013. Biosens. Bioelectron. 41, 669–674.

Zhang, X., Zhou, J., Zhang, C.D., Zhang, D.J., Su, X.R., 2016. RSC Adv. 6 (2), 1279–1287.

Zhao, Y.T., Yang, M.M., Fu, Q.Q., Ouyang, H., Wen, W., Song, Y., Zhu, C.Z., Lin, Y.H., Du, D., 2018. Anal. Chem. 90 (12), 7391–7398.

Zou, Z.X., Du, D., Wang, J., Smith, J.N., Timchalk, C., Li, Y.Q., Lin, Y.H., 2010. Anal. Chem. 82 (12), 5125–5133.